Trans. Tianjin Univ. 2015, 21: 140-146
DOI 10.1007/s12209-015-2584-8

Aircraft Landing Gear Control with Multi-Objective Optimization Using Generalized Cell Mapping*

Sun Jianqiao(孙建桥)[1,2], Jia Teng(贾　腾)[1], Xiong Furui(熊夫睿)[1],
Qin Zhichang(秦志昌)[1], Wu Weiguo(吴卫国)[1], Ding Qian(丁　千)[1]
(1. School of Mechanical Engineering, Tianjin University, Tianjin 300072, China;
2. School of Engineering, University of California, Merced, CA 95343, USA)

Abstract: This paper presents a numerical algorithm tuning aircraft landing gear control system with three objectives, including reducing relative vibration, reducing hydraulic strut force and controlling energy consumption. Sliding mode control is applied to the vibration control of a simplified landing gear model with uncertainty. A two-stage generalized cell mapping algorithm is applied to search the Pareto set with gradient-free scheme. Drop test simulations over uneven runway show that the vibration and force interaction can be considerably reduced, and the Pareto optimum form a tight range in time domain.

Keywords: landing gear; sliding mode control; model uncertainty; multi-objective optimization; generalized cell mapping

Landing gear dynamics and control have drawn attention from academia and industry for decades. Active and semi-active controls have been introduced to the landing gear system in order to reduce vibrations and landing gear-fuselage interactions, especially on uneven runway under combat situation. The dynamics and control issues in the landing gear system include vertical vibration and transverse skid[1]. Since the 1970s, National Aeronautics and Space Administration (NASA) has launched a series of programs to develop comprehensive vertical landing dynamic models[2]. Later, active and semi-active controls were introduced by adding a hydraulic energy absorbing system outside the gear stroke[3,4].

Most researches on the landing gear system make use of a simplified two degree-of-freedom (DOF) mass-spring-damper model, which shares many features with the automobile suspension system. In recent years, many control technologies initially used in the automobile industry have found their role in the active control design for landing gears, including magneto-rheological (MR) and electro-rheological (ER) dampers[5], feedback optimal controls[3,6], sliding mode controls[7] and passive optimal controls[8].

Multi-objective optimization of passive and active systems has attracted much attention[6,9,10]. Unlike traditional single-objective optimization problems (SOPs), the optimum solutions for multi-objective optimization problem (MOP) form a Pareto set.

The cell mapping methods introduced by Hsu[11] provided a robust and global algorithm for MOPs[12]. Two cell mapping methods were extensively studied, i.e., simple cell mapping (SCM) and generalized cell mapping (GCM)[11,13]. Crespo and Sun[14,15] studied the fixed final state optimal control problems, and applied the cell mapping methods to the optimal control of deterministic systems described by Bellman's principle of optimality[16].

In this paper, we will study the multi-objective optimal feedback control of a simplified landing gear model. The rest is outlined as follows: Section 1 presents the nonlinear dynamic model, proposes the sliding mode control and defines the multi-objective functions; Section 2 formulates the MOPs in general terms; Section 3 presents the GCM searching algorithm with gradient-free scheme; Section 4 gives the optimal results of landing gear feedback controller design together with the simulation results over uneven runway. The paper is closed in the final section.

Accepted date: 2014-12-15.
*Supported by the National Natural Science Foundation of China (No.11172197 and No.11332008) and a key-project grant from the Natural Science Foundation of Tianjin (No.010413595).
Sun Jianqiao, born in 1956, male, Dr, Prof.
Correspondence to Sun Jianqiao, E-mail: jsun3@ucmerced.edu.

1 Landing gear model

A simplified 2-DOF landing gear model is shown in Fig. 1.

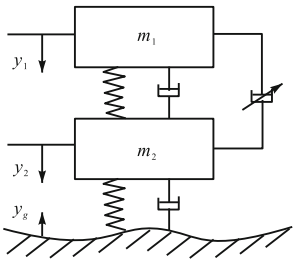

Fig. 1 Simplified 2-DOF landing gear model

The equations of motion are given as follows:

$$\begin{cases} m_1\ddot{y}_1 = m_1 g - F_a - F_l - f - F_Q \\ m_2\ddot{y}_2 = m_2 g + F_a + F_l + f + F_Q - F_t \end{cases} \tag{1}$$

where F_a is gas spring force; F_l the damping force; f the friction force; F_Q the active control force; and F_t the tire reaction force. The sum of F_a, F_l and f is called the strut force denoted as F_s, i.e., $F_s = F_a + F_l + f$. The strut force represents the landing gear-fuselage interaction, which is an important cause of fuselage fatigue and damage. The upper mass and lower mass are denoted as m_1 and m_2, respectively.

The expressions of all the forces are listed as below[4,17]:

$$F_a(y_s) = p_0 A\left(\frac{V_0}{V_0 - Ay_s}\right)^{\gamma} \tag{2}$$

$$F_l(y_s) = \frac{\rho A^3 \dot{y}_s |\dot{y}_s|}{2\varsigma^2 A_0^2} \tag{3}$$

$$f = F_f(\dot{y}_s) = k_m \dot{y}_s + k_n \dot{y}_s \operatorname{sgn}(\dot{y}_s) \tag{4}$$

$$F_t(y_2, \dot{y}_2) = k_t y_2 + c_t \dot{y}_2 \tag{5}$$

$$y_2^* = \frac{(m_1 + m_2)g}{k_t} \tag{6}$$

$$y_1^* = y_2^* + \frac{V_0}{A}\left[1 - \left(\frac{p_0 A}{m_1 g}\right)^{\frac{1}{\gamma}}\right] \tag{7}$$

where y_1^* and y_2^* are the static positions of the upper and lower masses, respectively; $y_s = y_1 - y_2$ the landing gear piston stroke; and $\dot{y}_s = \dot{y}_1 - \dot{y}_2$ the stroke velocity. The displacement of the system away from the equilibrium position are $\tilde{y}_1 = y_1 - y_1^*$ and $\tilde{y}_2 = y_2 - y_2^*$; p_0, V_0 and A are the initial pressure, initial volume and cross section area of the upper gas chamber, respectively; and ρ, ς and A_0 are the oil density, orifice discharge coefficient and orifice area of the oil damper, respectively; k_m and k_n are empirical parameters to model the damping-like friction; k_t and c_t are the spring and damper coefficients representing the tire reaction in Eq. (5) respectively. Eqs. (2)—(4) describe the nonlinear stiffness and damping terms of the landing gear system.

The active control force F_Q is given as[18],

$$F_Q = k_a \lambda u + k_b \lambda^2 u|u| \tag{8}$$

where k_a and k_b are experimentally determined coefficients; λ the flow rate; and u the control valve displacement. Note that u is the control command that we will design, while F_Q is the actual mechanical output of the control. We can treat F_Q as the system control input first. After F_Q is determined, we can find the control command u as follows:

$$u = \begin{cases} \dfrac{-k_a + \sqrt{k_a^2 + 4k_b F_Q}}{2\lambda k_b}, & F_Q > 0 \\ \dfrac{k_a - \sqrt{k_a^2 - 4k_b F_Q}}{2\lambda k_b}, & F_Q < 0 \end{cases} \tag{9}$$

Since the control input u is usually bounded above by u_{max}, which implies the limited capability of control units, the corresponding bounds on F_Q can be obtained and they are considered in the design of the optimal F_Q. The values of all system parameters mentioned here are listed in Tab. 1.

Tab. 1 Parameters used in landing gear model

Parameter	Value	Parameter	Value
p_0/Pa	1.6×10^6	c_t/(N·s·m^{-1})	2.6×10^4
A/m^2	1.376×10^{-2}	k_t/(N·m^{-1})	1.5×10^6
ς	0.3	k_m/(N·s·m^{-1})	7×10^3
V_0/m^3	6.88×10^{-3}	k_n/(N·s^2·m^{-2})	1×10^4
ρ/(kg·m^{-3})	912	k_a/(N·m^{-1})	3.35×10^6
m_1/kg	4 832.7	k_b/(N·m^{-2})	4.37×10^6
m_2/kg	145.1	u_{max}/m	8×10^{-3}
g/(kg·m^{-2})	9.81	γ	1.865
A_0/m^2	6.412×10^{-4}	λ	2.85

1.1 Sliding model control design

Note that the gas spring force given in Eq. (2) is so complicated that it is hard to perform a stability analysis. One practical way to model gas spring force is data fitting. To avoid the fitting error, sliding mode control is applied to tackle the model uncertainty. To steamline the application of sliding mode control, we treat data generated from Eq. (2) as the experimental data and use curve fitting to model the gas spring force.

Let the piston stroke be $y_s = y_s^* + \tilde{y}_s$, where $\tilde{y}_s$ is

the stroke away from the static position y_s^*. The gas spring force is decomposed at y_s^*, i.e., $F_a(y_s)=F_a(y_s^*)+\tilde{F}_a(\tilde{y}_s)$, where $\tilde{F}_a(0)=0$. Since $F_a(y_s^*)$ is the gas spring force at static position, it is a constant. Let $\hat{F}_a(\tilde{y}_s)$ be the curve fitting approximation of $\tilde{F}_a(\tilde{y}_s)$. We propose a third order polynomial of $\hat{F}_a(\tilde{y}_s)$, i.e.,

$$\hat{F}_a(\tilde{y}_s)=p_1\tilde{y}_s^3+p_2\tilde{y}_s^2+p_3\tilde{y}_s \tag{10}$$

The fitting results are $p_1=1.424\times10^6$, $p_2=8.061\times10^5$ and $p_3=2.191\times10^5$. Fig. 2 shows the comparison of fitting result of Eq. (10) and data generated from Eq. (2). Note that the range of $\tilde{y}_s$ can largely influence the fitting parameters, and in this paper it is set as $[0,10\text{ cm}]$.

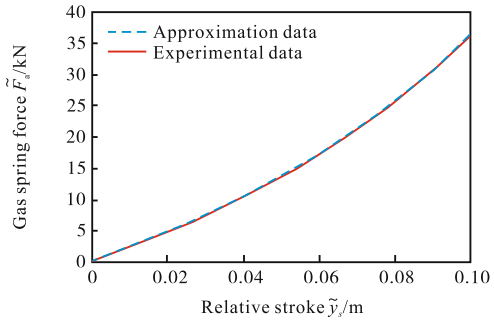

Fig. 2 Curve fitting of nonlinear gas spring force $\hat{F}_a$ versus the real $\tilde{F}_a$ described in Eq. (2)

The equations of motion are as follows,

$$\begin{cases} m_1\ddot{\tilde{y}}_1=-\tilde{F}_a-\left[\dfrac{\rho A^3}{2\varsigma^2A_0^2}+k_n\right]\dot{\tilde{y}}_s\left|\dot{\tilde{y}}_s\right|-k_m\dot{\tilde{y}}_s-F_Q \\ m_2\ddot{\tilde{y}}_2=\tilde{F}_a+\left[\dfrac{\rho A^3}{2\varsigma^2A_0^2}+k_n\right]\dot{\tilde{y}}_s\left|\dot{\tilde{y}}_s\right|+k_m\dot{\tilde{y}}_s-k_t\tilde{y}_2-c_t\dot{\tilde{y}}_2+F_Q \end{cases} \tag{11}$$

To handle the model uncertainty brought by $\tilde{F}_a$, the sliding surface is proposed as $s=\dot{\tilde{y}}_s+\lambda\tilde{y}_s$, with $\lambda>0$ guaranting the asymptotic behavior once the system is on the sliding surface. The upper bound of estimation error of $\tilde{F}_a$ is denoted as F_e, i.e., $\left|\tilde{F}_a(\tilde{y}_s)-\hat{F}_a(\tilde{y}_s)\right|<F_e$. The feedback control law is as follows,

$$F_Q=\frac{m_1}{m_1+m_2}(k_t\tilde{y}_2+c_t\dot{\tilde{y}}_2)-\hat{F}-\frac{\lambda m_1m_2}{m_1+m_2}\dot{\tilde{y}}_s-K\text{sat}\left(\frac{s}{\Phi}\right) \tag{12}$$

where $\hat{F}=\hat{F}_a(\tilde{y}_s)+F_l(\dot{\tilde{y}}_s)+F_f(\dot{\tilde{y}}_s)$ is the estimated strut force with respect to static position y_s^*; K the switching gain; Φ the boundary layer width to avoid chattering; and sat( ) the saturation function. By choosing the Lyapunov function as $V=\frac{1}{2}s^2$, it is easy to prove that the closed loop system is asymptotically stable if $K>F_e$. The sliding mode control design involves three free parameters remaining to be tuned, i.e., λ, K and Φ.

Note that the curve fitting of Eq. (10) directly influences the upper bound of error estimation and the lower bound of switching gain K. To evaluate the upper bound of model uncertainty brought by F_e, we simply use the maximum absolute fitting error as the indicator,

$$\left|\tilde{F}_a(\tilde{y}_s)-\hat{F}_a(\tilde{y}_s)\right|<F_e=\max_{\tilde{y}_s\in U}\left|\tilde{F}_a(\tilde{y}_s)-\hat{F}_a(\tilde{y}_s)\right| \tag{13}$$

Note that the fitting error is sensitive to the fitting range U, which is usually limited by hardware capability or physical conditions. The gas spring fitting error is 0.087.

1.2 Performance indices

The major objectives of active control of landing gear are to reduce relative upper mass vibration $\tilde{y}_1$, hydraulic strut force F_s and control energy consumption. With fixed structural parameters, controller tuning becomes the only way to achieve the optimization over several objectives. To measure the overall performance, two integrals are introduced. The maximum strut force over the short dropping phase in $t\in[0,T_f]$ is used to measure the control effort on force reduction. Usually, the impacting phase during landing is short. In our simulation, we take $T_f=2$ s. The input-output function values of Eq. (14) are evaluated by conducting a drop test to flat ground with initial impact velocity $v_0=2.5$ m/s.

$$\boldsymbol{F}(\boldsymbol{k})=\left[F_1,F_2,F_3\right]^{\mathrm{T}}=\left[\int_0^{T_f}\tilde{y}_1^2\mathrm{d}t,\int_0^{T_f}u^2\mathrm{d}t,F_{s,\max}\right]^{\mathrm{T}} \tag{14}$$

2 Multi-objective optimization

The MOP can be expressed as follows:

$$\min_{\boldsymbol{x}\in B}\{\boldsymbol{F}(\boldsymbol{x})\} \tag{15}$$

where F is the map that consists of the objective functions $f_i:B\to\mathbf{R}$, i.e.,

$$\boldsymbol{F}:B\to\mathbf{R}^p$$
$$\boldsymbol{F}(\boldsymbol{x})=(f_1(\boldsymbol{x}),\cdots,f_k(\boldsymbol{x})) \tag{16}$$

The domain $B\subset\mathbf{R}^q$ of $\boldsymbol{F}$ can be expressed as below:

$$B=\{\boldsymbol{x}\in\mathbf{R}^q\mid g_i(\boldsymbol{x})\leqslant0,\ i=1,\cdots,l,\text{ and }h_j(\boldsymbol{x})=0,\ j=1,\cdots,m\} \tag{17}$$

In this paper, we will only consider the inequality constraints.

Next, we have to define the optimal solutions of a given MOP using the concept of dominance[19].

Let $\boldsymbol{v}, \boldsymbol{w} \in \mathbf{R}^p$. Then $\boldsymbol{v} <_p \boldsymbol{w}$, if $v_i < w_i$ for all $i \in \{1, \cdots, k\}$. The relation $\leqslant_p$ is defined analogously.

A vector $\boldsymbol{y} \in B$ is called dominated by a vector $\boldsymbol{x} \in B (\boldsymbol{x} \prec \boldsymbol{y})$ with respect to Eq. (15) if $\boldsymbol{F}(\boldsymbol{x}) \leqslant_p \boldsymbol{F}(\boldsymbol{y})$ and $\boldsymbol{F}(\boldsymbol{x}) \neq \boldsymbol{F}(\boldsymbol{y})$, else $\boldsymbol{y}$ is called non-dominated by $\boldsymbol{x}$.

If $\boldsymbol{x}$ dominates $\boldsymbol{y}$, then $\boldsymbol{x}$ can be considered to be better according to the given MOP. The definition of optimality of a given MOP is now straightforward $\boldsymbol{x}$.

A point $\boldsymbol{x} \in B$ is called (Pareto) optimal or a Pareto point of Eq. (15), if there is no $\boldsymbol{y} \in B$ that dominates .

The set of all Pareto optimal solutions is called Pareto set, i.e.,

$$\mathscr{P} := \{x \in B: x \text{ is a Pareto point of Eq. (16)}\} \quad (18)$$

The image $\boldsymbol{F}(\mathscr{P})$ of $\mathscr{P}$ is called the Pareto front.

Pareto set and Pareto front typically form $(p-1)$-dimensional objects under certain mild assumptions on the MOP[20]. Recent studies with the SCM indicate the existence of fine structures of Pareto front [21].

3 Searching algorithm

3.1 Generalized cell mapping and gradient-free search

GCM allows the existence of multiple image cells compared with its SCM counterpart. In GCM, the mappings are stored in a sparse logical matrix, which is a directed graph. Alternatively, one can use a list to store GCM. Let $\boldsymbol{G} \in \mathbf{R}^{N_c \times N_c}$ denote the GCM representation, where N_c is the total number of cells in the cell space. If cell $\boldsymbol{z}_j$ is an image of $\boldsymbol{z}_i$, then $\boldsymbol{G}(i, j) = 1$; otherwise, $\boldsymbol{G}(i, j) = 0$.

The introduction of GCM compensates the discrete error caused by cell mapping to some extent, especially when the cell size is large for coarsely divided cell space. Usually, the construction of GCM is obtained by sampling test points within a pre-image cell[22]. For gradient-free searching in MOP[21,23], where no dynamical system is involved, GCM is built by accepting all dominating neighbor cells.

In gradient-free search, the images of cell $\boldsymbol{z}$ are selected by comparing the function values among all its adjacent cells. Let $\boldsymbol{z}^N$ denote the adjacent cell set that surrounds $\boldsymbol{z}$. If there exists at least one cell in $\boldsymbol{z}^N$ with all function values lower than $\boldsymbol{z}$, i.e., $\boldsymbol{z}_j^N$ dominates $\boldsymbol{z}$, then we pick $\boldsymbol{z}_j^N$ as one of the image cells of $\boldsymbol{z}$. If no adjacent cells dominate cell $\boldsymbol{z}$, then here are three possibilities: Case 1, cell $\boldsymbol{z}$ is a Pareto optimum if it is not located in the taboo region defined by Eq. (16) for constrained optimization; Case 2, $\boldsymbol{z}$ is optimal at local scale but its optimality is not guaranteed over the entire parameter space; Case 3, cell $\boldsymbol{z}$ itself is located in T and is designated as a sink cell with its image cell also being designated as sink. By convention, we denote sink cell with zero as its index. In this way, the gradient-free GCM $\boldsymbol{G}$ can be built very quickly since there is no involvement of gradient associated calculation. The searching in cell space can be performed in an iterative manner until the accuracy criteria is met at a fine cellular space resolution. In this paper, we use the two-stage cell mapping with one subdivision.

3.2 Dominance check

The basic principle of dominance check is the Pareto optimality defined in Section 2, i.e., if cell $\boldsymbol{z}_i < \boldsymbol{z}_j$, then $\boldsymbol{z}_j$ will be eliminated from the acquired set. The complexity of dominance check is $O(N \lg N)$, where N is the number of cells in the set[24]. To speed up the comparison procedure, we first sort the first objective of all cells in an ascending order. Knowing that the first cell after sorting must stay in the set, we start from the second cell. For each cell $\boldsymbol{z}_i$ under processing, we store the kept cells that survive the dominance check in set S_k, and perform the comparison between $\boldsymbol{z}_i$ and each cell in S_k in a reversed order, i.e., the local comparison is conducted from larger to smaller for the first objective. In this regard, the local comparison time of each cell stays at a minimum level. Once a cell $\boldsymbol{z}_j \in S_k$ outperforms $\boldsymbol{z}_i$, the comparison is stopped and $\boldsymbol{z}_i$ is ruled out. The whole process lasts from $\boldsymbol{z}_2$ to $\boldsymbol{z}_N$.

4 Numerical results

We take the structural parameters of the landing gear model[18], and all parameters appearing in Section 1 are listed in Tab. 1. The searching region is set as $Q = [1,10] \times [0.5,1.5] \times [0.01 \times 0.5]$ for tuning parameter vector $\boldsymbol{k} = [K, \lambda, \Phi]^{\mathrm{T}}$. The searching bound is selected based upon system stability and maximum model uncertainty. Note that in Section 1, the upper bound of modelling error is estimated as 0.087. It is also shown that the model uncertainty upper bound serves as the lower bound for switching gain K. Hence, the lower bound of K is set as 1 during the optimization process to remove the effect of model uncertainty. The performance constraints are im-

posed as $\int_0^{T_f}\tilde{y}_1^2\mathrm{d}t<2.5, \int_0^{T_f}u^2\mathrm{d}t<1.5\times10^{-3}$ and $F_{s,max}<140$.

The initial cell space partition is [10×10×10], which resulting in 144 coarse cells. A refinement with [3×3×3] partition among resulting cells in the first stage is taken for the second stage. In total, 1 429 cells are found within the refined cell space, and 371 cells left after dominance check are performed to eliminate the faked Pareto cells. The entire optimization costs 641.221 9 s under MATLAB environment. Figs. 3 and 4 show the Pareto set and Pareto front acquired via the two-stage GCM searching. The conflicting nature among optimization objectives can be clearly observed from Fig. 4. Note that for both passive and active controlled landing gear systems, the amount of kinematic energy that the system absorbs remains nearly at a constant level. Hence, the general relationship between landing gear vibration and strut force should be inversely proportional; on the other hand, the introduction of external control units shares the functionality of oleo-pneumatic shock strut force with certain amount of control effort. To ensure the vibration suppression in terms of upper mass displacement, quite amount of control energy should be devoted to balance the contribution between the active control force and damping strut force.

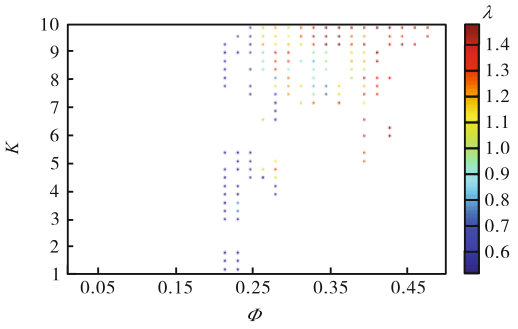

(a) Pareto set with third parameter λ

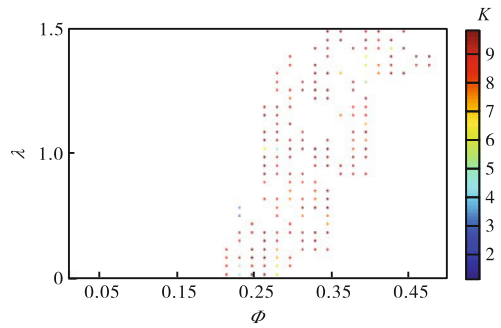

(b) Pareto set with third parameter K

Fig. 3 Pareto set found after two-stage generalized cell mapping searching

To test the control effect of the acquired optimal solutions, we conduct a drop test simulation for all Pareto optimal solutions in time domain. Note that the parameter tuning using cell mapping algorithm is carried out by simulating a drop test without a bump. To simulate the uneven runway, we use half sine wave function. The runway excitation will last for 0.4 s and it is assumed to have the form as below:

$$y_g=0.1\sin\frac{2\pi}{0.8}t \tag{19}$$

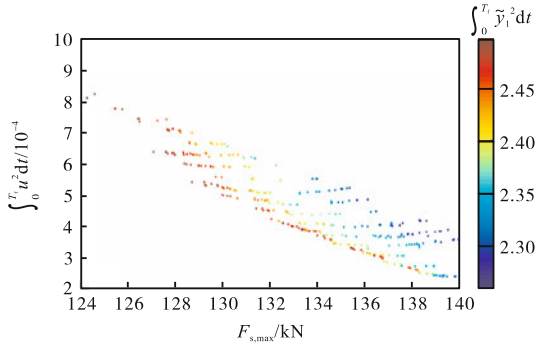

(a) Pareto front of the landing gear MOP with third objective $\int_0^{T_f}\tilde{y}_1^2\mathrm{d}t$

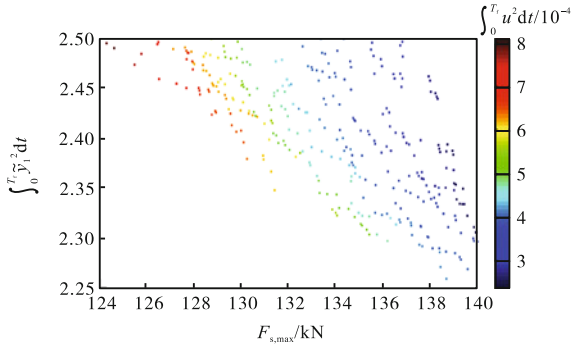

(b) Pareto front of the landing gear MOP with third objective $\int_0^{T_f}u^2\mathrm{d}t$

Fig. 4 Pareto front of the landing gear MOP in correspondence with the Pareto set shown in Fig. 3

Figs. 5—7 demonstrate the control effect over three objectives defined in Eq. (14). Drop tests are simulated with the initial impact velocity $v_0=2.5$ m/s. The parameter vector $\boldsymbol{k}=[K,\lambda,\Phi]^{\mathrm{T}}$ with each performance index as minimum values are $[9.950\,0,1.383\,3,0.295\,8]^{\mathrm{T}}$, $[9.250\,0,0.616\,7,0.214\,2]^{\mathrm{T}}$ and $[9.550\,0,1.350\,0,0.475\,5]^{\mathrm{T}}$. The corresponding Pareto fronts $\boldsymbol{F}(\boldsymbol{k})=\left[\int_0^{T_f}\tilde{y}_1^2\mathrm{d}t,\int_0^{T_f}u^2\mathrm{d}t,F_{s,max}\right]^{\mathrm{T}}$ among these parameter vectors are $[2.258\,1,4.130\,1\times10^{-4},138.644\,9]^{\mathrm{T}}$, $[2.304\,5,2.375\,0\times10^{-4},139.875\,3]^{\mathrm{T}}$ and $[2.493\,3,8.055\,9\times10^{-4},124.289\,1]^{\mathrm{T}}$. The performance index of $\int_0^{T_f}\tilde{y}_1^2\mathrm{d}t$ and $F_{s,max}$ are 2.284 0 and 155.071 4 for uncontrolled system. Apparently, the feedback controlled system outperforms the uncontrolled system, especially for

the significant reduction of hydraulic strut force. In addition, it can be seen from Figs. 5 and 6 that the transient processes of violent vibration end faster than uncontrolled system when the optimal controller design is integrated.

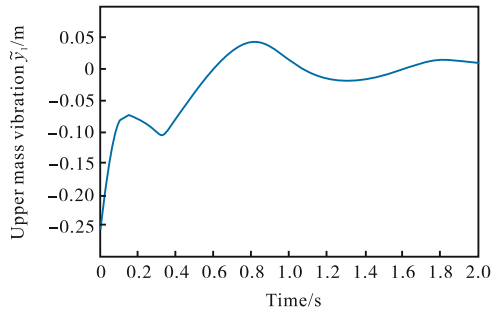

(a) Response of $\tilde{y}_1$ without control

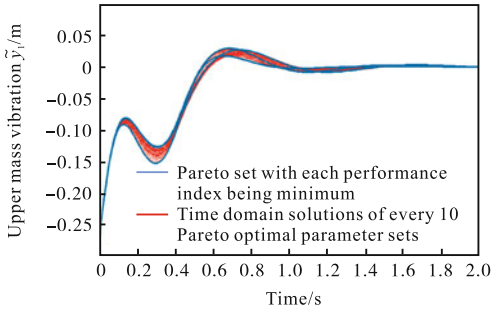

(b) Response of $\tilde{y}_1$ with control, where extremas roughly define time domain boundary of Pareto set

Fig. 5 Response of $\tilde{y}_1$

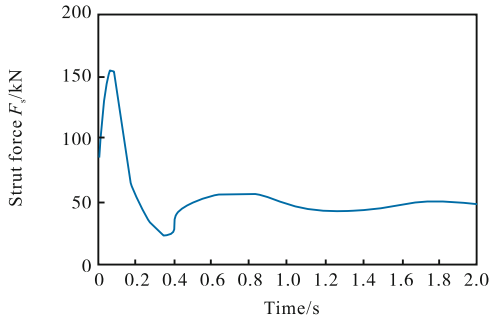

(a) Response of F_s without control

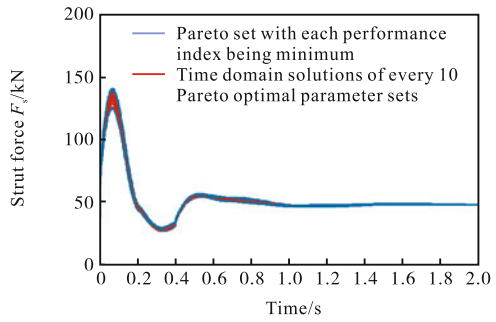

(b) Response of F_s with control, where extremas roughly define time domain boundary of Pareto set

Fig. 6 Response of F_s

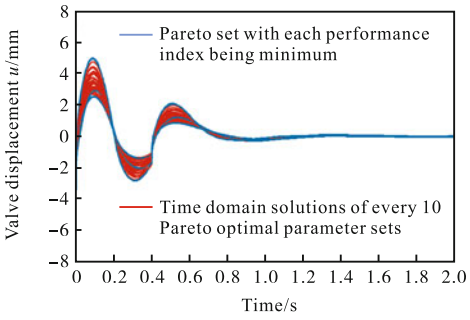

Fig. 7 Valve displacements with control

5 Conclusions

This paper studies the active control of a 2-DOF landing gear model with multiple optimization objectives taken into consideration. A two-stage generalized cell mapping algorithm with gradient-free searching is proposed to find the Pareto set in cellular space, and a fast dominance check algorithm is used to eliminate the fake Pareto cells caused by discrete error. Drop test simulations over uneven runway are conducted to test the optimization effects. It is found that the extrema of Pareto optimum roughly define the boundaries of temporal responses of all candidate optimal solutions.

References

[1] Pritchard J. Overview of landing gear dynamics[J]. *Journal of Aircraft*, 2001, 38 (1): 130-137.

[2] McGehee J R, Carden H D. A Mathematical Model of an Active Control Landing Gear for Load Control During Impact and Roll-Out[R]. Technical Note TN D-8080. NASA, USA, 1976.

[3] Vu K. Advances in Optimal Active Control Techniques for Aerospace Systems: Application to Aircraft Active Landing Gear[D]. University of California, Los Angeles, USA, 1989.

[4] Wang H T, Xing J T, Price W G *et al*. An investigation of an active landing gear system to reduce aircraft vibrations caused by landing impacts and runway excitations[J]. *Journal of Sound and Vibration*, 2008, 317(1/2): 50-66.

[5] Yao G Z, Yap F F, Chen G *et al*. MR damper and its application for semi-active control of vehicle suspension system[J]. *Mechatronics,* 2002, 12(7): 963-973.

[6] Gao H J, Lam J, Wang C H. Multi-objective control of vehicle active suspension systems via load-dependent controllers[J]. *Journal of Sound and Vibration*, 2006, 290(3-5): 654-675.

[7] Sam Y M, Osman J H S, Ghani M R A. A class of proportional-integral sliding mode control with application to active suspension system[J]. *Systems & Control Letters*, 2004, 51(3/4): 217-223.

[8] Goga V, Klucik M. Optimization of vehicle suspension parameters with use of evolutionary computation[J]. *Procedia Engineering*, 2012, 48: 174-179.

[9] Brown M, Smith R E. Directed multi-objective optimization[J]. *International Journal of Computers*, *Systems and Signal*, 2005, 6(1): 3-17

[10] Maciejewski I. Control system design of active seat suspensions[J]. *Journal of Sound and Vibration*, 2012, 331(6): 1291-1309.

[11] Hsu C S. *Cell-to-Cell Mapping*: *A Method of Global Analysis for Nonlinear Systems*[M]. Springer-Verlag, New York, USA, 1987.

[12] Hernández C, Naranjani Y, Sardahi Y *et al*. Simple cell mapping method for multi-objective optimal feedback control design[J]. *International Journal of Dynamics and Control*, 2013, 1(3): 231-238.

[13] Hsu C S. A theory of cell-to-cell mapping dynamical systems[J]. *Journal of Applied Mechanics*, 1980, 47:931-939.

[14] Crespo L G, Sun J Q. Solution of fixed final state optimal control problems via simple cell mapping[J]. *Nonlinear Dynamics*, 2000, 23(4): 391-403.

[15] Crespo L G, Sun J Q. Optimal control of target tracking with state constraints via cell mapping[J]. *Journal of Guidance*, *Control*, *and Dynamics*, 2001, 24(5): 1029-1031.

[16] Crespo L G, Sun J Q. Fixed final time optimal control via simple cell mapping[J]. *Nonlinear Dynamics*, 2003, 31(2): 119-131.

[17] Liu H, Gu H B, Chen D W. Application of high-speed solenoid valve to the semi-active control of landing gear[J]. *Chinese Journal of Aeronautics*, 2008, 21(3): 232-240.

[18] Horta L G, Daugherty R H, Martinson V J. Modeling and Validation of a Navy A6-Intruder Actively Controlled Landing Gear System[R]. Report TP-1999-209124. NASA, USA, 1999.

[19] Pareto V. *Manual of Political Economy*[M]. Augustus M Kelley, New York, USA, 1971.

[20] Hillermeier C. *Nonlinear Multiobjective Optimization: A Generalized Homotopy Approach*[M]. Birkhauser, Berlin, Germany, 2001.

[21] Naranjani Y, Hernández C, Xiong F R *et al*. A hybrid algorithm for the simple cell mapping method in multi-objective optimization[C]. In: *EVOLVE International Conference*. Leiden, The Netherland, 2013.

[22] Hsu C S. A discrete method of optimal control based upon the cell state space concept[J]. *Journal of Optimization Theory and Applications*, 1985, 46(4): 547-569.

[23] Xiong F R, Qin Z C, Xue Y *et al*. Multi-objective optimal design of feedback controls for dynamical systems with hybrid simple cell mapping algorithm[J]. *Communications in Nonlinear Science and Numerical Simulation*, 2014, 19(5): 1465-1473.

[24] Kung H T, Luccio F, Preparata F P. On finding the maxima of a set of vectors[J]. *Journal of the ACM*, 1975, 22(4): 469-476.

(Editor: Wu Liyou)